熱プラズマに関する研究

プラズマジェット等のプラズマ応用における基礎的研究がメイン.

具体的には,

・熱プラズマにおける熱流動特性に関する理論, 及び実験的研究

・プラズマ診断 ……瞬間的にプラズマの温度を測定することができるプローブ法の開発と熱流体計測

以下, 概要を示す.

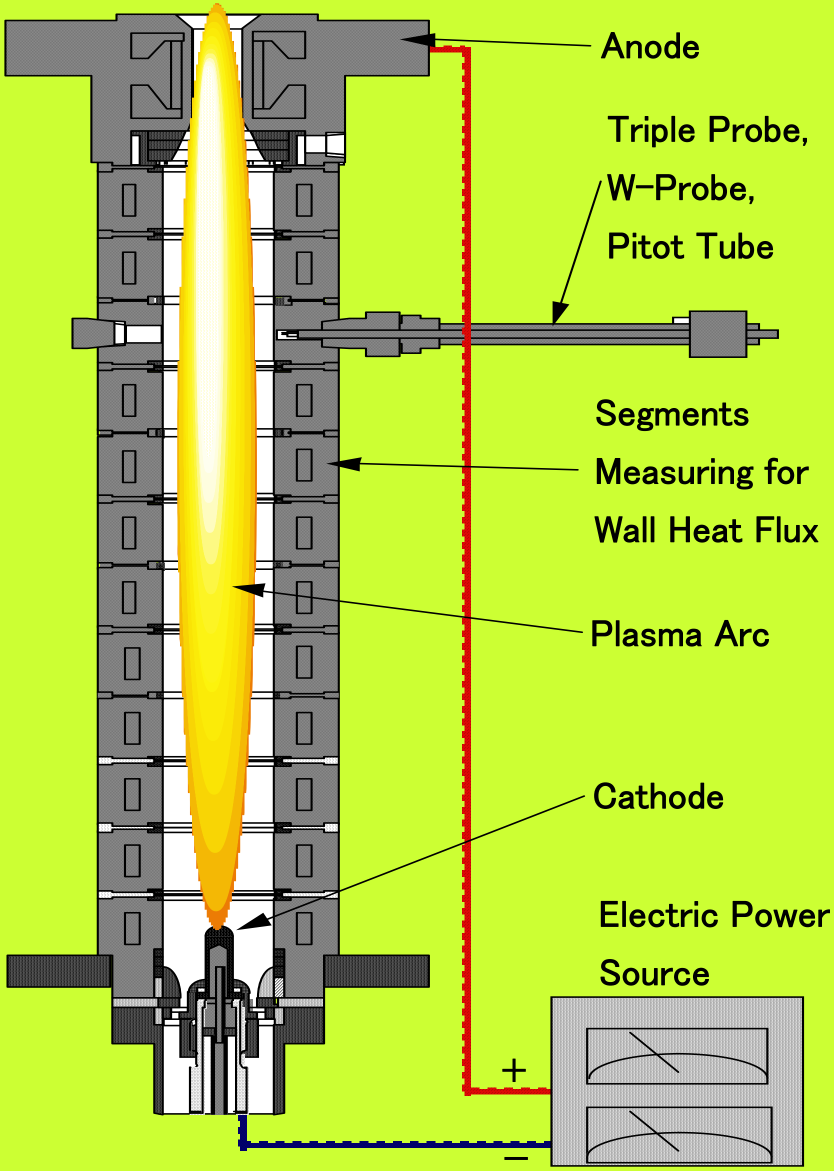

Diameter d_o=40 mm

Distance between cathode and anode L=360 mm

Ar gas

Mass flow rate m_G=1.25, 2.5, 5.0 g/s

D.C. current I_{plasma}=200 A, 250 A

Voltage 200V

FIG. 1 Schematic diagram of the experimental apparatus of the plasma torch of an arc plasma generator.

Plasma temperature : Triple probe method

5000K

$\lambda_D = 6.439 \times 10^{-6}$ m, $\lambda_e = 1.142 \times 10^{-6}$ m, $r_p = 2.50 \times 10^{-4}$ m

$\lambda_D > \lambda_e$, $r_p > \lambda_e$ (continuum plasma)

10000K

$\lambda_D = 2.732 \times 10^{-8}$ m, $\lambda_e = 2.283 \times 10^{-6}$ m

$r_p > \lambda_e > \lambda_D$

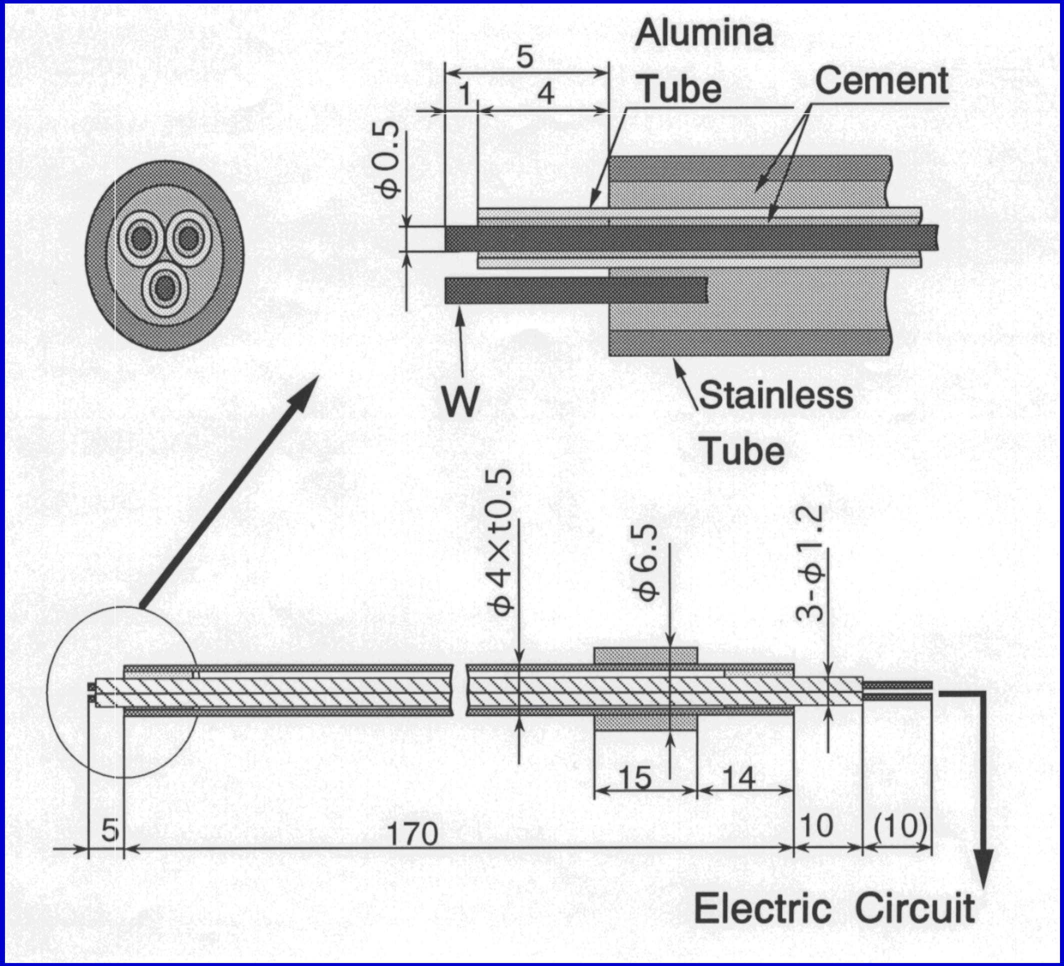

$$\frac{2I_{p2}+I_{p3}}{I_{p2}+2I_{p3}}=\frac{1-\exp\left(-e\Delta V_2/k_B T_e\right)}{1-\exp\left(-e\Delta V_3/k_B T_e\right)}$$

FIG. 2 Schematic diagram of the triple probe.

,

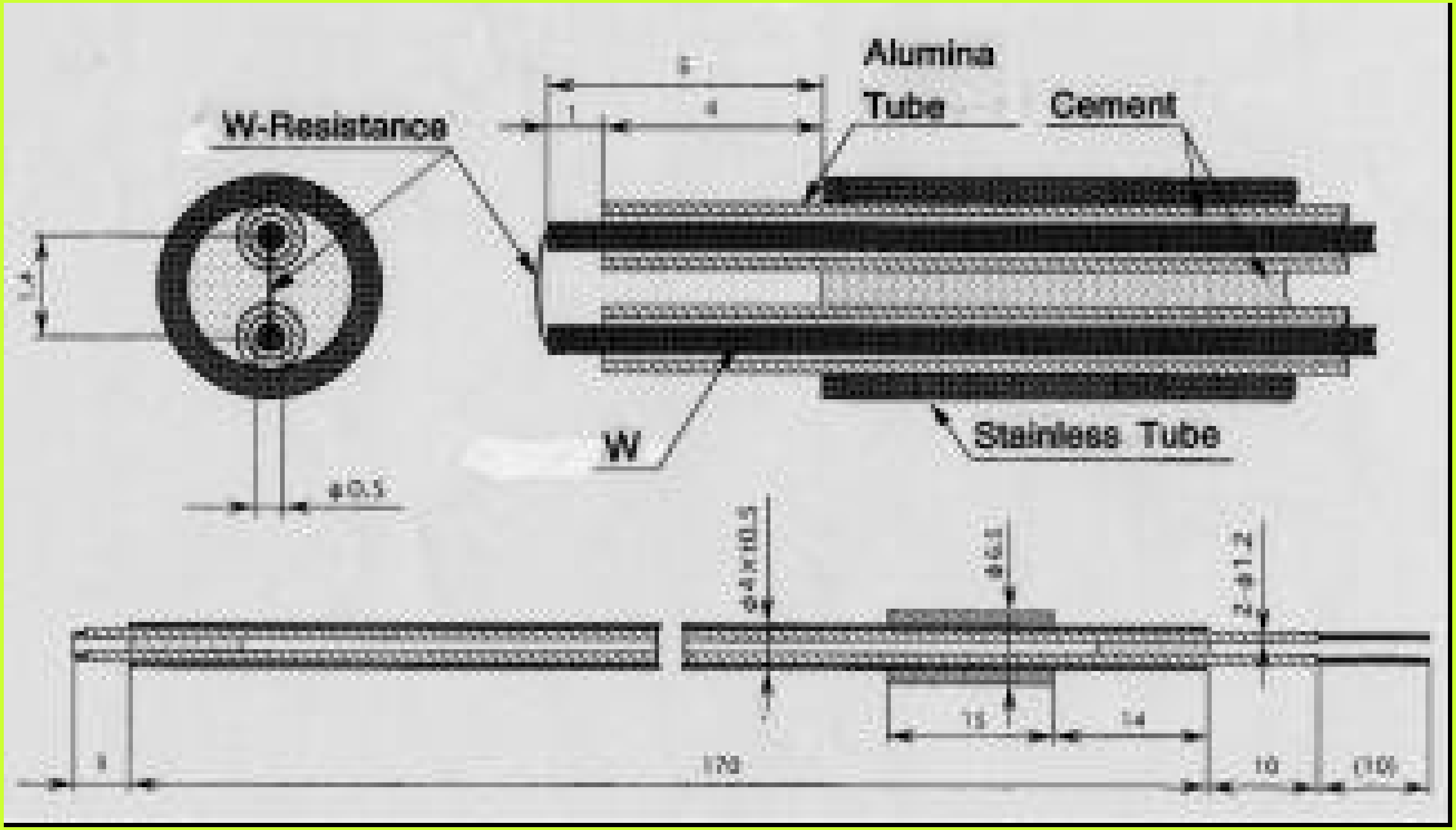

$$T_W = \frac{-\alpha + \sqrt{\alpha^2 - 4\beta\gamma}}{2\beta} \qquad \gamma = 1 - \frac{\sigma_W}{\sigma_{oo}}$$

FIG. 3 Schematic diagram of the W-probe.

Plasma velocity

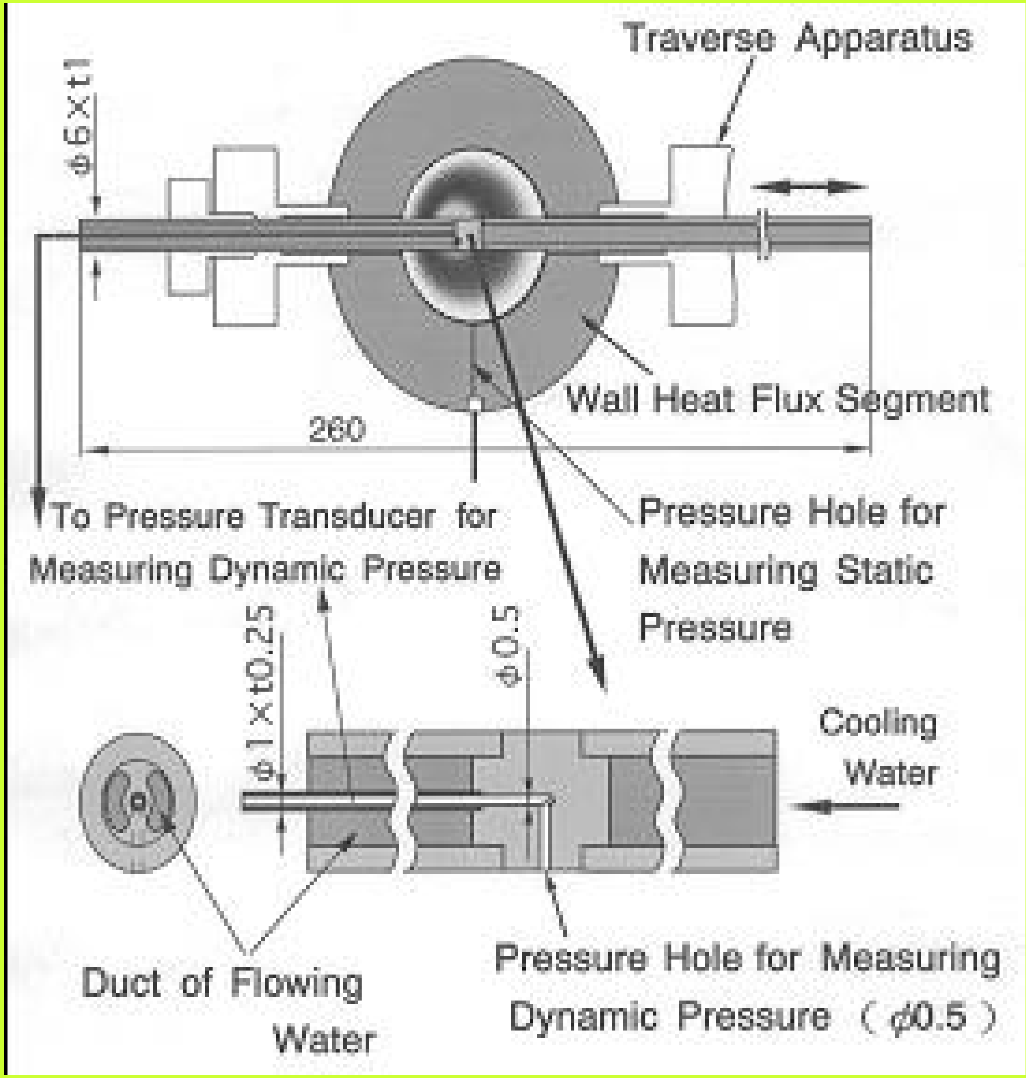

$$v = c\sqrt{\frac{2\Delta p}{\rho}}$$

FIG. 4 Schematic diagram of the pitot tube and settlement in the segment.

Mean enthalpy

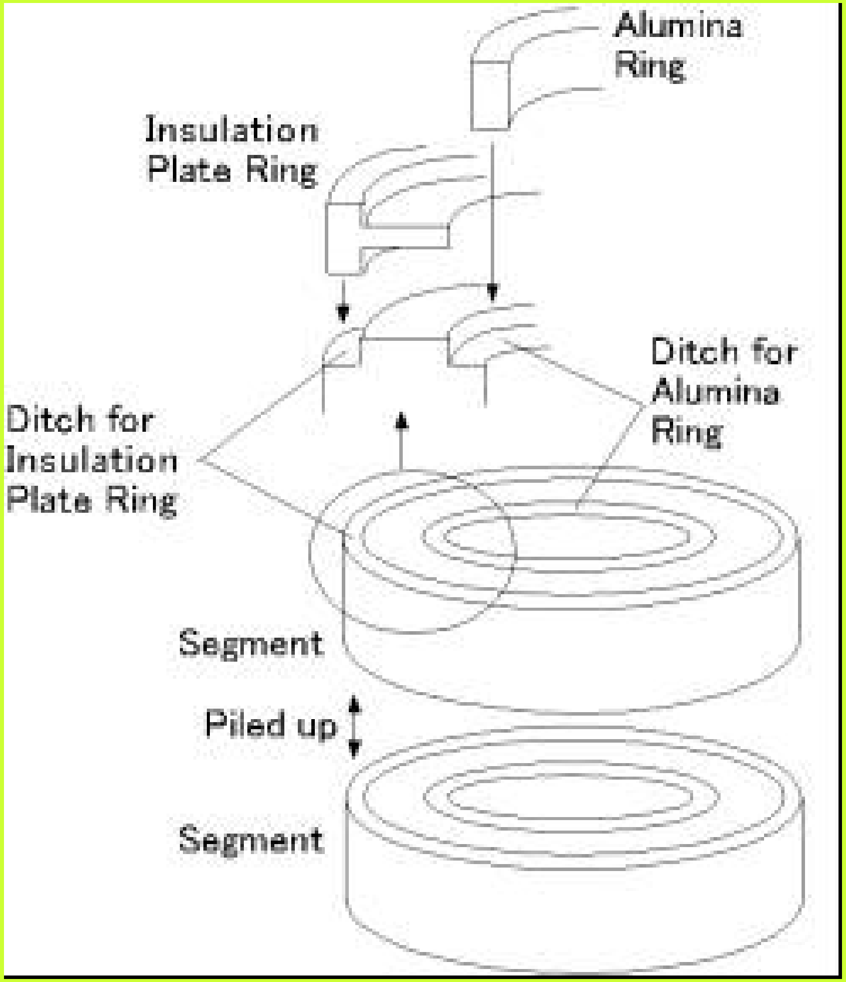

$$h_{pm} = \frac{1}{m_G}\int_0^{r_0} q_p 2\pi r dr$$

$$q_p = c_p m_G T_p$$

$$h_{p,n} = h_{p,n-1} + \frac{(1-L_{n-1})Q_{E,n} + L_n Q_{E,n+1} - Q_{L,n}}{m_G}$$

$$L_n = \ell_n / (\ell_n + \ell_{n+1})$$

$$Q_{E,n} = (E_n - E_{n-1}) I_{plasma}$$

$$Q_{L,n} = c_{pL,n} \rho_{w,n} V_{c,n} \Delta T_n$$

FIG. 5 Schematic diagram of a segment for measuring heat flux in the plasma torch.

I_{plasma}=200 A, m_G=2.5 g/s
h_{pm}=1765.6 kJ/kg
$h_{p,10}$=1910.9 kJ/kg

I_{plasma}=200 A, m_G=5.0 g/s
h_{pm}=1130.9 kJ/kg
$h_{p,10}$=1393.1 kJ/kg

I_{plasma}=200 A, m_G=1.25 g/s
h_{pm}=3231.5 kJ/kg
$h_{p,10}$=2839.5 kJ/kg.

Numerical simulation

$$\frac{\partial}{\partial z^*}\left(r^*\rho^* v_z^*\right)+\frac{\partial}{\partial r^*}\left(r^*\rho^* v_r^*\right)=0$$

$$\frac{\partial}{\partial z^*}\left\{r^*\left(\rho^* v_z^* v_r^* - \frac{\mu^*}{\mathrm{Re}}\frac{\partial v_r^*}{\partial z^*}\right)\right\}+\frac{\partial}{\partial r^*}\left\{r^*\left(\rho^* v_r^* v_r^* - \frac{\mu^*}{\mathrm{Re}}\frac{\partial v_r^*}{\partial r^*}\right)\right\}$$

$$=-r^*\frac{\partial p^*}{\partial r^*}+\frac{\partial}{\partial z^*}\left(r^*\frac{\mu^*}{\mathrm{Re}}\frac{\partial v_z^*}{\partial r^*}\right)+\frac{\partial}{\partial r^*}\left(r^*\frac{\mu^*}{\mathrm{Re}}\frac{\partial v_r^*}{\partial r^*}\right)$$

$$-2\frac{\mu^*}{\mathrm{Re}}\frac{v_r^*}{r^*}-\frac{\mathrm{Re}_m N_{oh}^{-1}}{\pi^2 N_p}r^* J_z^* B_\theta^*$$

$$\frac{\partial}{\partial z^*}\left\{r^*\left(\rho^* v_z^* v_z^* - \frac{\mu^*}{\mathrm{Re}}\frac{\partial v_z^*}{\partial z^*}\right)\right\}+\frac{\partial}{\partial r^*}\left\{r^*\left(\rho^* v_r^* v_z^* - \frac{\mu^*}{\mathrm{Re}}\frac{\partial v_z^*}{\partial r^*}\right)\right\}$$

$$=-r^*\frac{\partial p^*}{\partial z^*}+\frac{\partial}{\partial z^*}\left(r^*\frac{\mu^*}{\mathrm{Re}}\frac{\partial v_z^*}{\partial z^*}\right)+\frac{\partial}{\partial r^*}\left(r^*\frac{\mu^*}{\mathrm{Re}}\frac{\partial v_r^*}{\partial z^*}\right)$$

$$+\frac{\mathrm{Re}_m N_{oh}^{-1}}{\pi^2 N_p}r^* J_r^* B_\theta^*$$

$$\frac{\partial}{\partial z^*}\left\{r^*\left(c_p^*\rho^* v_z^* T^* - \frac{k^*}{\mathrm{RePr}}\frac{\partial T^*}{\partial z^*}\right)\right\} + \frac{\partial}{\partial r^*}\left\{r^*\left(c_p^*\rho^* v_r^* T^* - \frac{k^*}{\mathrm{RePr}}\frac{\partial T^*}{\partial r^*}\right)\right\}$$

$$= \frac{16 N_{oh}^{-1}}{\pi^2\,\mathrm{RePr}}\frac{r^*\left(J_z^{*2} + J_r^{*2}\right)}{\sigma^*} - \frac{N_p}{\mathrm{RePr}} r^* Ra^*$$

$$B_\theta^* = \frac{4\mu_m^*}{r^*}\int_0^{r^*} r^* J_z^* dr^*$$

$$E_z^* = \frac{I^*}{8\int_0^{0.5} r^* \sigma^* dr^*}$$

$$\frac{\partial}{\partial z^*}\left(r^* J_z^*\right) + \frac{\partial}{\partial r^*}\left(r^* J_r^*\right) = 0$$

Boundary condition

at the inlet of the plasma torch

$$v_z^* = 1, \quad v_r^* = 0, \quad T^* = 0,$$

at the cathode

$$J_z^* = 1, \quad J_r^* = 0,$$

at the outlet of the plasma torch

$$\frac{\partial v_z^*}{\partial z^*} = \frac{\partial v_r^*}{\partial z^*} = 0, \quad \frac{\partial T^*}{\partial z^*} = 0, \quad \frac{\partial J_z^*}{\partial z^*} = J_r^* = 0,$$

at the wall

$$v_z^* = v_r^* = 0, \quad T^* = 0, \quad J_z^* = J_r^* = 0,$$

at the axis of the plasma torch

$$\frac{\partial v_z^*}{\partial r^*} = v_r^* = 0, \quad \frac{\partial T^*}{\partial r^*} = 0, \quad \frac{\partial J_z^*}{\partial r^*} = J_r^* = 0$$

Plasma temperature

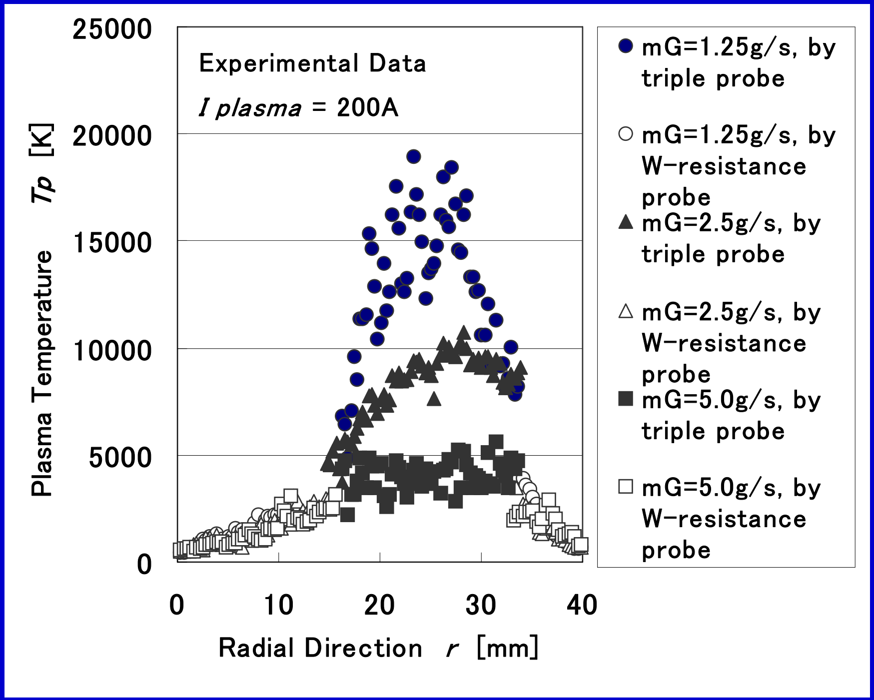

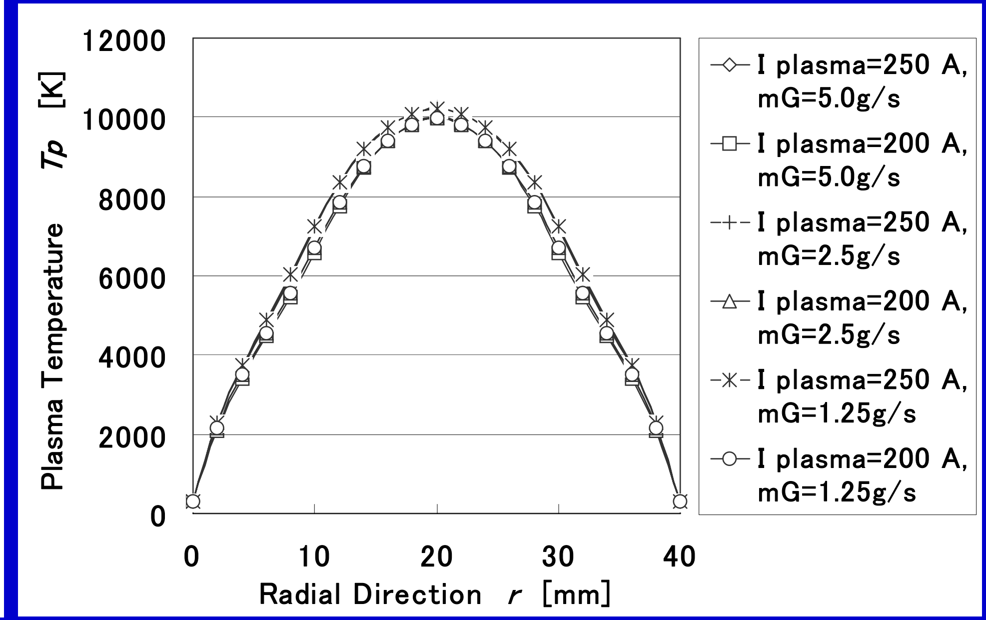

(a) experimental results

(b) numerical results

FIG. 6 A comparison of plasma temperature between the experimental and numerical results.

Plasma velocity

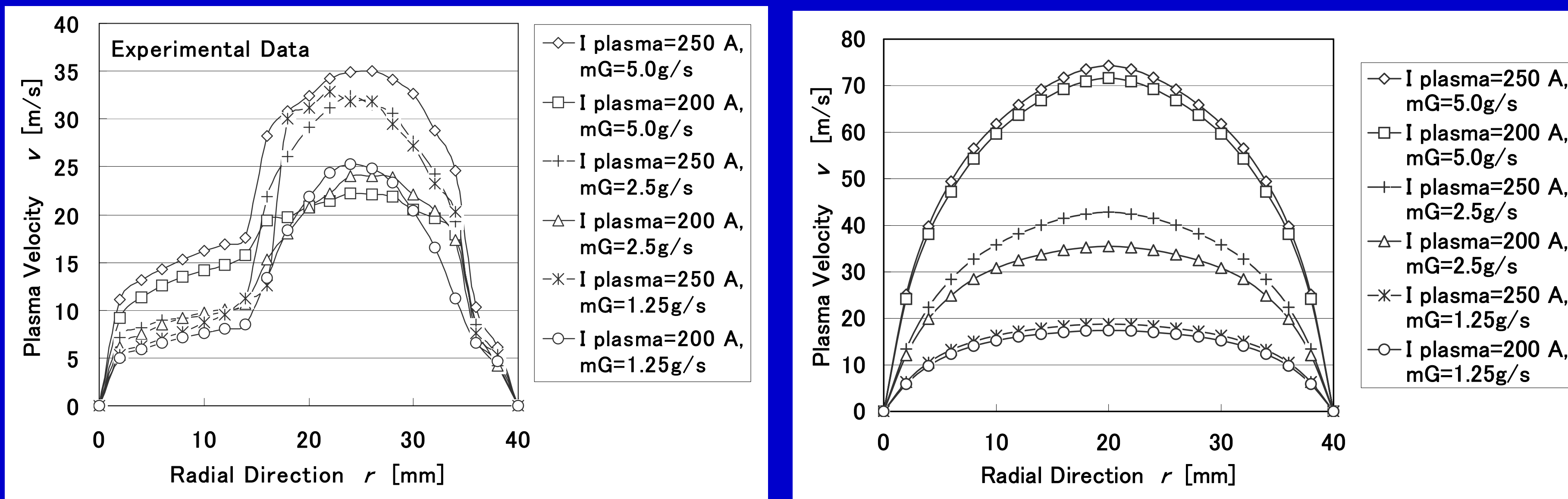

(a) experimental results　　(b) numerical results

FIG. 7 A comparison of plasma temperature between the experimental and numerical results.

Current density

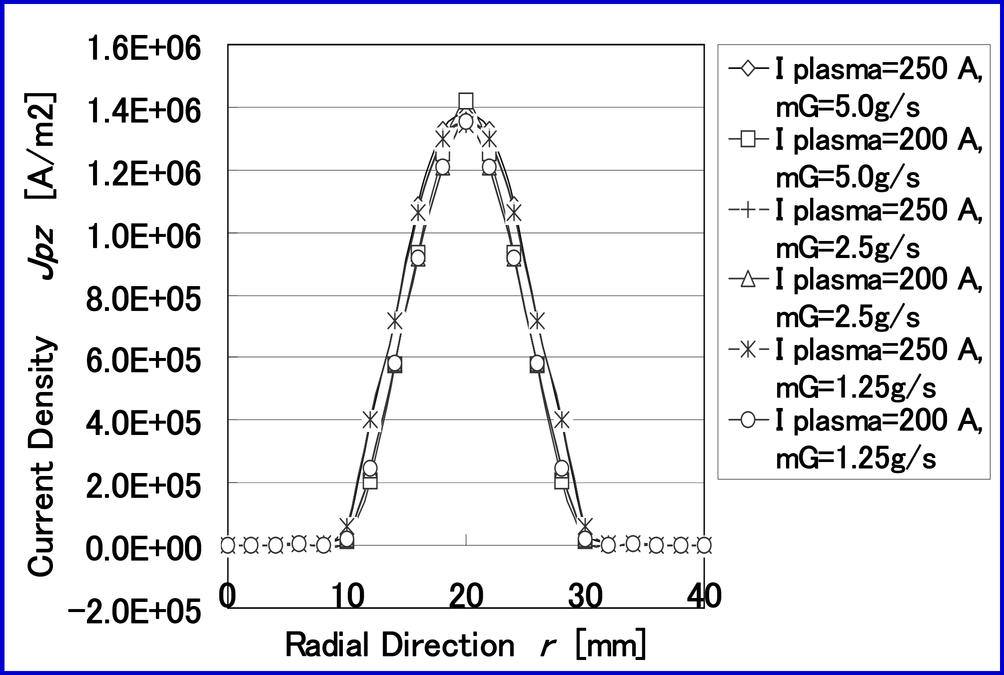

Fig. 8 Numerical results for the plasma current density.